



Formation of amides from alcohols and amines using maghemite-copper oxide nanocomposite as catalyst

Hassan Hassani^{*a} and Foad Shaghayeghi Toosi^b

^aDepartment of Chemistry, Payame Noor University, 19395-4697 Tehran, I. R. of Iran

E-mail: hassaniir@yahoo.com

^bDepartment of Chemistry, Payame Noor University, Mashhad, I. R. of Iran

Manuscript received online 18 September 2019, revised 23 September 2019, accepted 24 September 2019

Maghemite-copper oxide nanocomposite structure was synthesized and characterized with X-ray diffraction (XRD), Inductively Coupled Plasma (ICP), electron microscopy techniques (SEM and TEM), vibrational sampling magnetometer (VSM). This system was applied as a catalyst for optimization and the amidation of benzyl alcohol with benzyl amine. We have developed the amide bond formation from alcohols and amines using TBHP as an oxidant with high selectivity and in high yields using γ -Fe₂O₃@CuO composite. A wide variety of amines has been tested (primary and secondary, aniline and amino acids) and shown good activity in this reaction.

This method have several advantages, including high yield, simple work-up and recyclable property of the catalyst. The catalyst can be readily isolated by using an external magnet and no obvious loss of activity was observed when the catalyst was reused in five consecutive runs.

Keywords: Nanocatalyst, direct amidation, maghemite-copper oxide.

Introduction

The amide bond plays a key role in organic and biological chemistry. The most common traditional method for the synthesis of the amides is treatment of activated carboxylic acid derivatives with amines¹⁻³. The amide bond is a ubiquitous functionality found in a wide range of chemical structures, including biomolecules, natural products, pharmaceuticals, and polymers^{4,5}. Amide bond formation has been one of the most important transformations in organic synthesis and a various methods have been reported⁶. Recently, a highly atom economical and environmentally benign method, transition metal catalyzed amide synthesis directly from alcohols and amines, was highlighted. Direct amidation of alcohols with amines have been developed with precious transition metals (e.g. Ru, Rh, Re and Au)⁷⁻¹³. However, high reaction temperature, oxidant, and solvent, were normally required in order to gain good result. Direct amidation process of alcohol requires the catalyst to affect the oxidation of both the alcohol to aldehyde and the hemiaminal intermediate formed between aldehyde and amine to produce

amide^{14,17}. Copper compounds are particularly attractive catalysts for such a transformation because they are inexpensive and low toxic (permitted daily exposure limit >13 mg)¹⁸⁻²¹. In addition, they have been shown to catalyze the oxidation of alcohols to aldehydes and aldehydes to amides. Copper oxide has been a hot topic among the studies on transition metal oxides because of its interesting properties^{22,23}. MOFs with nano-sized features and supramolecular structures are ideal candidates for precursors in solid state calcination processes to fabricate nano-sized metal and metal oxides with novel structures and properties²⁴. CuO nanostructures with the large surface area and size effects possess superior physical and chemical properties that remarkably different from those of their bulk counterparts. The application of magnetic nanoparticles (MNPs) as catalysts is attractive because of their high surface area, unique magnetic properties and high catalytic activity. We report the demonstration of γ -Fe₂O₃@CuO as catalyst for the synthesis of amides from benzylic alcohols and hydrochloric salts of amines. Magnetic γ -Fe₂O₃@CuO nanocomposite with a core/shell structure was synthesized in direct calcinations of

magnetic $\gamma\text{-Fe}_2\text{O}_3$ @HKUST-1 in air atmosphere similar to of Fe_3O_4 @CuO method with some modification²⁵.

Experimental

Chemicals: All reagents were purchased from Merck and Sigma-Aldrich and used without further purification. Products were characterized by comparison physical data with known samples and spectroscopic data (FT-IR, ^1H NMR, and ^{13}C NMR). The NMR spectra were recorded on a Bruker Avance DPX 500 MHz instrument. The spectra were measured in DMSO.

FT-IR spectra were recorded on a JASCO FT-IR 460 plus spectrophotometer. Powder X-ray diffraction data were collected on a Holland Philips X'pert instrument using Co-K α as X-ray source. SEM images of the catalyst were obtained on a KYKY-EM3200 device and a homemade vibrating sample magnetometer (VSM) was used for measuring magnetic properties of the catalyst. Melting points were determined in open capillaries with a Buchi 510 melting point apparatus.

Catalyst preparation:

Preparation of $\gamma\text{-Fe}_2\text{O}_3$ @CuO:

The $\gamma\text{-Fe}_2\text{O}_3$ @CuO nanocomposite was synthesized, according to the literature¹⁶ with some modifications to get $\gamma\text{-Fe}_2\text{O}_3$ instead of Fe_3O_4 .

First step: A solution containing 0.86 g $\text{FeCl}_2\cdot 4\text{H}_2\text{O}$ and 2.34 g $\text{FeCl}_3\cdot 6\text{H}_2\text{O}$ were dissolved in deionized water (85 mL) under Ar atmosphere at room temperature. To this solution, was added dropwise NH_3 (aq.) solution (25%, w/w, 30 mL) to reach the reaction pH to 11. This black dispersion then heated to reflux for 1 h. The magnetic nanoparticles were then washed 3 times with deionized water. Finally, the precipitates were dried at 140°C for 24 h to get $\gamma\text{-Fe}_2\text{O}_3$.

Second step: 0.05 g synthesized $\gamma\text{-Fe}_2\text{O}_3$ was mixed with 10 mL of ethanol solution of mercaptoacetic acid (MAA) (0.29 mM) and stirred for 25 h. The product was recovered by an external magnetic field and washed with distilled water and ethanol. 0.05 g of MAA-functionalized $\gamma\text{-Fe}_2\text{O}_3$ core synthesized, was dispersed in 4 mL of $\text{Cu}(\text{CH}_3\text{COO})_2\cdot \text{H}_2\text{O}$ ethanol solution (10 mM) for 15 min and then with 4 mL of benzenetricarboxylic acid ethanol solution (10 mM) for 30 min at 40°C. Washed with ethanol and dried under vacuum at 150°C, then was calcined up to 600°C in air atmosphere after 5 h. The yield of catalyst finally was 72%.

Results and discussion

Catalyst characterization:

The XRD spectra of $\gamma\text{-Fe}_2\text{O}_3$ and $\gamma\text{-Fe}_2\text{O}_3$ @CuO is shown in Fig. 1. The XRD patterns confirm the conversion of $\gamma\text{-Fe}_2\text{O}_3$ to $\gamma\text{-Fe}_2\text{O}_3$ @CuO.

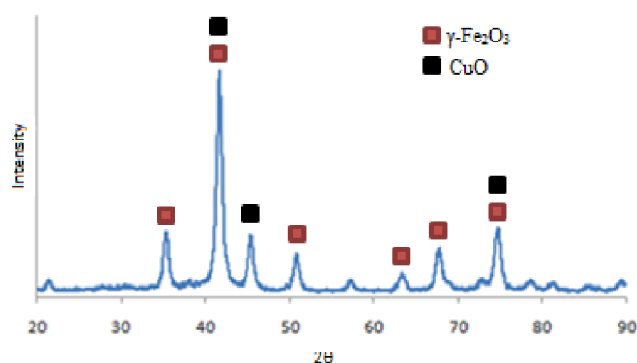


Fig. 1. The X-ray diffraction patterns of the $\gamma\text{-Fe}_2\text{O}_3$ and $\gamma\text{-Fe}_2\text{O}_3$ @CuO.

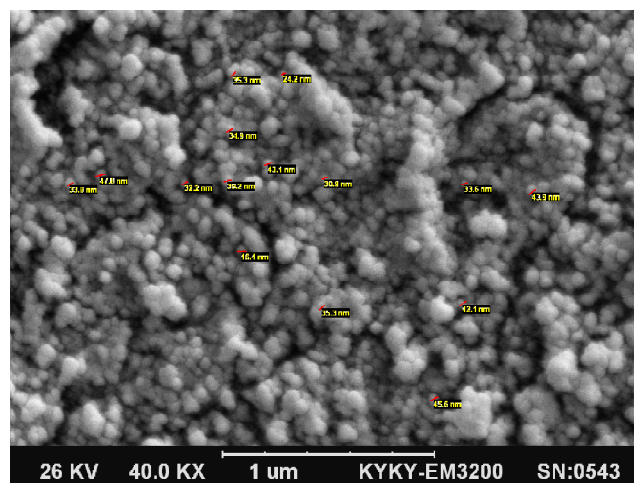


Fig. 2. SEM image of the $\gamma\text{-Fe}_2\text{O}_3$ and $\gamma\text{-Fe}_2\text{O}_3$ @CuO.

Diffraction peaks at around 35°, 51°, 63°, 68° and 75° are related to $\gamma\text{-Fe}_2\text{O}_3$ and peaks at 45° and 75° corresponded to CuO. No peaks of impurity are found in the XRD pattern. The average size of the nanoparticles was measured using Scherrer's formula: $D = 0.9\lambda/\beta \cos \theta$, D is the average crystalline size, λ is the X-ray wavelength ($\alpha = 1.78897 \text{ \AA}$), β is the angular line width of half-maximum intensity and θ is Bragg's angle in degree. The mean nanoparticle diameter

for bare Fe_3O_4 is 50 nm. We investigated the morphology, size and structure of nano $\gamma\text{-Fe}_2\text{O}_3\text{@CuO}$ using scanning electron microscopy (SEM) (Fig. 2). The TEM result showed that the nanocomposite material included a $\gamma\text{-Fe}_2\text{O}_3$ core and a CuO shell (Fig. 3). Magnetization measurements as a function of magnetic field were made on nano $\gamma\text{-Fe}_2\text{O}_3\text{@CuO}$. Saturation magnetization is 48.8 emu/g. Also, according to curve, Mr/Ms is 0.02 that demonstrates superparamagnetivity of nanoparticles (Fig. 4).



Fig. 3. TEM image of $\gamma\text{-Fe}_2\text{O}_3\text{@CuO}$ nanocomposite.

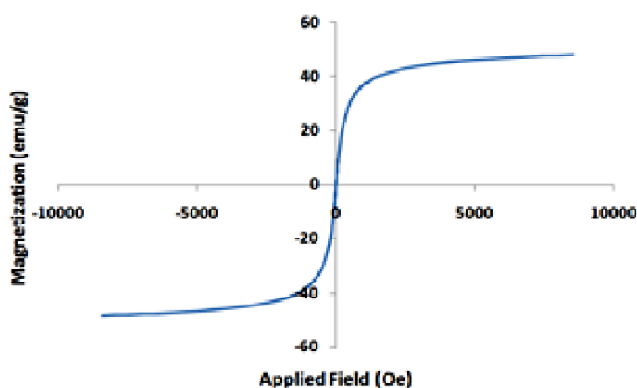


Fig. 4. Magnetization curve of the $\gamma\text{-Fe}_2\text{O}_3\text{@CuO}$.

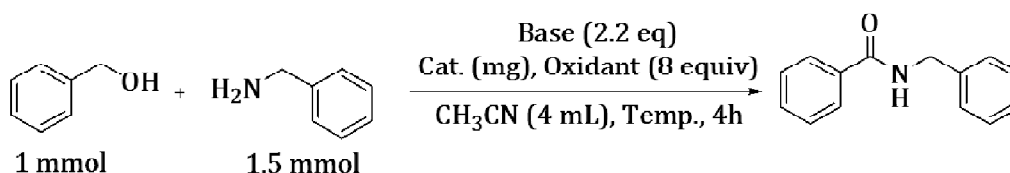
Inductively Coupled Plasma-Atomic Adsorption Spectroscopy (ICP-AAS) elemental analysis exhibited excellent detection for Cu and Fe. In order to determination of the amount of this elemental, the catalyst was dissolved in nitric acid. Finally Cu and Fe content were determined 15% and 55.4%, respectively.

Catalytic activity:

By considering the amidation of benzyl alcohol with benzyl amine as a model reaction (Scheme 1), a series of reaction conditions were optimized (Table 1).

We have changed the type of catalyst, the amount of catalyst, base, solvent and temperature in this reaction and the results below table was achieved (Table 1). We found that treating of benzyl alcohol (0.75 mmol) with hydrochloric salt of benzyl amine (0.5 mmol), TBHP (*tert*-butyl hydroperoxide) as the oxidant (8 equiv.), CaCO_3 as base (2.2 equiv.), at 80°C in acetonitrile (4 ml) for 6 h gave the best result, furnishing benzamide1e as the product in 91% yield (Table 1, entry 11).

The results of optimizing catalyst showed in this reaction Fe_3O_4 could catalyze this amidation but the reaction yield was unsatisfactory (Table 1, entry 1). To improve, other catalysts such as $\gamma\text{-Fe}_2\text{O}_3$ and $\gamma\text{-Fe}_2\text{O}_3\text{@CuO}$ were tested. In the presence of $\gamma\text{-Fe}_2\text{O}_3\text{@CuO}$, the yield increased to 70% (Table 1, entry 3). The yield of benzamide was up to 91% from 70% when the reaction temperature was decreased to 80°C from 100°C . We found that 80°C gave the best result (Table 1, entries 9–11). Several solvents were tested by using 20 mg $\gamma\text{-Fe}_2\text{O}_3\text{@CuO}$ as the catalyst and TBHP as the oxidant (Table 1, entries 11–15), acetonitrile proved to be the best medium for this reaction (Table 1, entry 11). After that, we attempted to use various oxidant, including TBHP, mCPBA (*meta*-chloroperoxybenzoic acid), H_2O_2 (hydrogen peroxide), NaOCl (sodium hypochlorite) and oxidant-free condition (Table 1, entries 11, 16, 17, 18, 25), and TBHP showed the highest yield (Table 1, entry 11). Meanwhile in



Scheme 1. Synthesis of benzylbenzamide in presence of $\gamma\text{-Fe}_2\text{O}_3\text{@CuO}$.

Table 1. Optimization of reaction conditions^a

Entry	Catalyst	Additive (mg)	Cat.	Oxidant	Base	Temp. (°C)	Solvent	Yield ^d (%)
1	Fe ₃ O ₄	–	20	TBHP	CaCO ₃	100	Acetonitrile	34
2	γ-Fe ₂ O ₃	–	20	TBHP	CaCO ₃	100	Acetonitrile	40
3	γ-Fe ₂ O ₃ @CuO	–	20	TBHP	CaCO ₃	100	Acetonitrile	70
4	γ-Fe ₂ O ₃ @CuO	–	20	TBHP	Na ₂ CO ₃	100	Acetonitrile	46
5	γ-Fe ₂ O ₃ @CuO	–	20	TBHP	K ₂ CO ₃	100	Acetonitrile	22
6	γ-Fe ₂ O ₃ @CuO	–	20	TBHP	NaOH	100	Acetonitrile	30
7	γ-Fe ₂ O ₃ @CuO	–	20	TBHP	KOH	100	Acetonitrile	29
8	γ-Fe ₂ O ₃ @CuO	–	20	TBHP	Et ₃ N	100	Acetonitrile	20
9	γ-Fe ₂ O ₃ @CuO	–	20	TBHP	CaCO ₃	40	Acetonitrile	45
10	γ-Fe ₂ O ₃ @CuO	–	20	TBHP	CaCO ₃	60	Acetonitrile	73
11	γ-Fe₂O₃@CuO	–	20	TBHP	CaCO₃	80	Acetonitrile	93
12	γ-Fe ₂ O ₃ @CuO	–	20	TBHP	CaCO ₃	80	EtOAc	45
13	γ-Fe ₂ O ₃ @CuO	–	20	TBHP	CaCO ₃	80	THF	63
14	γ-Fe ₂ O ₃ @CuO	–	20	TBHP	CaCO ₃	80	Dioxane	49
15	γ-Fe ₂ O ₃ @CuO	–	20	TBHP	CaCO ₃	80	CH ₂ Cl ₂	21
16	γ-Fe ₂ O ₃ @CuO	–	20	H ₂ O ₂	CaCO ₃	80	Acetonitrile	63
17	γ-Fe ₂ O ₃ @CuO	–	20	<i>m</i> CPBA	CaCO ₃	80	Acetonitrile	30
18	γ-Fe ₂ O ₃ @CuO	–	20	NaOCl	CaCO ₃	80	Acetonitrile	49
19	γ-Fe ₂ O ₃ @CuO	–	10	TBHP	CaCO ₃	80	Acetonitrile	38
20	γ-Fe ₂ O ₃ @CuO	–	25	TBHP	CaCO ₃	80	Acetonitrile	92
21	γ-Fe ₂ O ₃ @CuO	O-phen ^b	20	TBHP	CaCO ₃	80	Acetonitrile	50
22	γ-Fe ₂ O ₃ @CuO	Pyridine	20	TBHP	CaCO ₃	80	Acetonitrile	43
23	γ-Fe ₂ O ₃ @CuO	AcAc ^c	20	TBHP	CaCO ₃	80	Acetonitrile	32
24	γ-Fe ₂ O ₃ @CuO	–	–	TBHP	CaCO ₃	80	Acetonitrile	<10
25	γ-Fe ₂ O ₃ @CuO	–	20	–	CaCO ₃	80	Acetonitrile	–

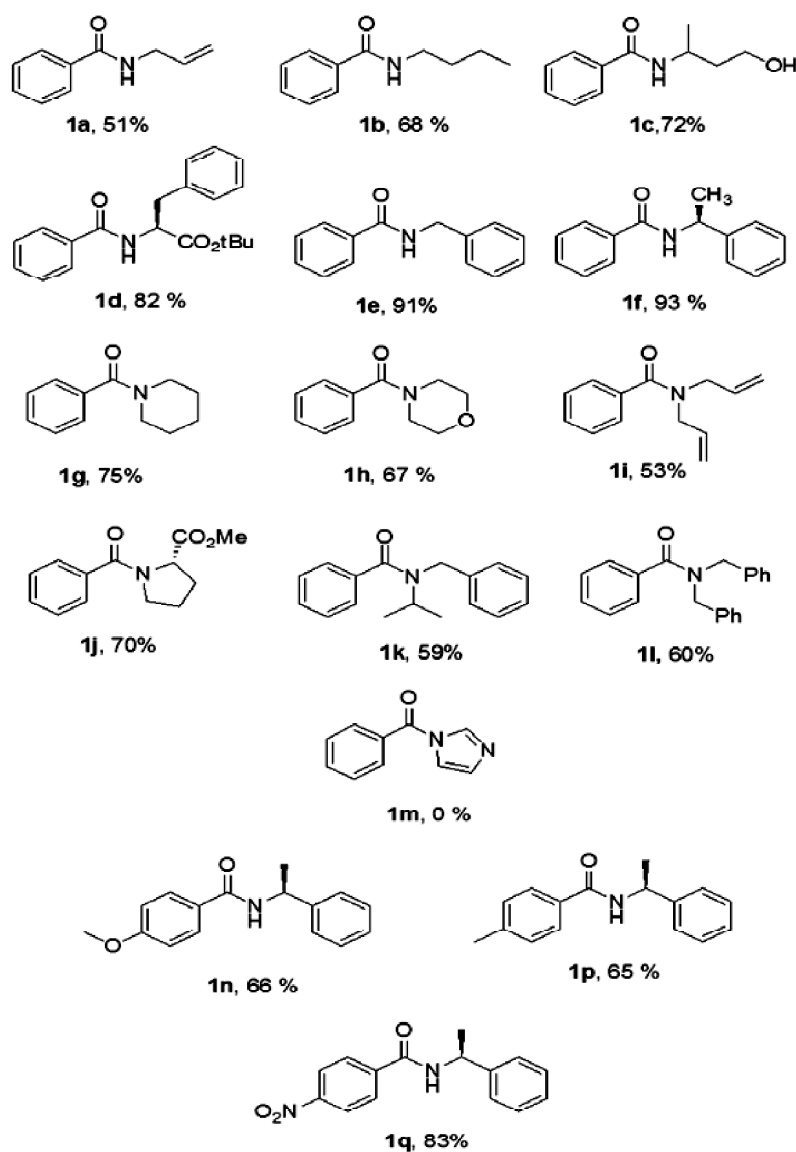
^aReactions were performed with benzyl alcohol (0.75 mmol), hydrochloride salt of benzyl amine (0.5 mmol), CH₃CN (4 ml), oxidant (8 equiv.), base (2.2 equiv.), at 80°C for 6 h, ^b1,10-phenanthroline, ^cacetylacetone, ^disolated yield.

absence of any oxidant, no amide formation was observed (Table 1, entry 25). Variation of the amounts of catalyst showed that the amide yield didn't increase with an increasing amount of γ-Fe₂O₃@CuO (Table 1, entry 20). Surprisingly, when the amount of catalyst was reduced, amide formation decreased significantly (Table 1, entry 19). After screening a variety of additives, the introduction of an additive did not improve the oxidative amidation reaction (Table 1, entries 21–23).

Under this optimized conditions, the substrate scope of this reaction was explored with various amine hydrochloride salts (aliphatic and aromatic) and benzyl alcohols (Table 2).

As can be seen in Table 2, aliphatic amines such as allyl, butyl amine and 2-amino-1-butanol were converted into their

corresponding amides in moderate to good yield (respectively 51%, 68% and 72%). Notably, no oxidation was observed in alcoholic function in **1c**. By using phenyl alanine *tert*-butyl ester as amine corresponding amide (**1d**) was isolated in 82% yield. The reaction worked well with benzyl amine and (s)-α-methyl benzyl amine, providing amides in excellent yields (**1e** and **1f**). Gratifyingly, the reaction with secondary amine salts (cyclic, aliphatic and aromatic amines) afforded the corresponding tertiary amides in moderate to good yields (**1g-l**). In the case of imidazole, the reaction was troublesome and no amide was detected (**1m**). We then screened some various benzyl alcohols in this reaction (**1n-q**) and α-methylbenzylamine was chosen as amine source. The benzyl alcohols with an electron-withdrawing group gave higher yields relative to the benzyl alcohols with an electron-

Table 2. Preparation of various benzamides in presence of $\gamma\text{-Fe}_2\text{O}_3\text{@CuO}^a$ 

^aReaction conditions: alcohol (0.75 mmol), hydrochloride salt of amine (0.5 mmol), TBHP (8 equiv.), CaCO_3 (2.2 equiv.), $\gamma\text{-Fe}_2\text{O}_3\text{@CuO}$ (20 mg), at 80°C for 6 h

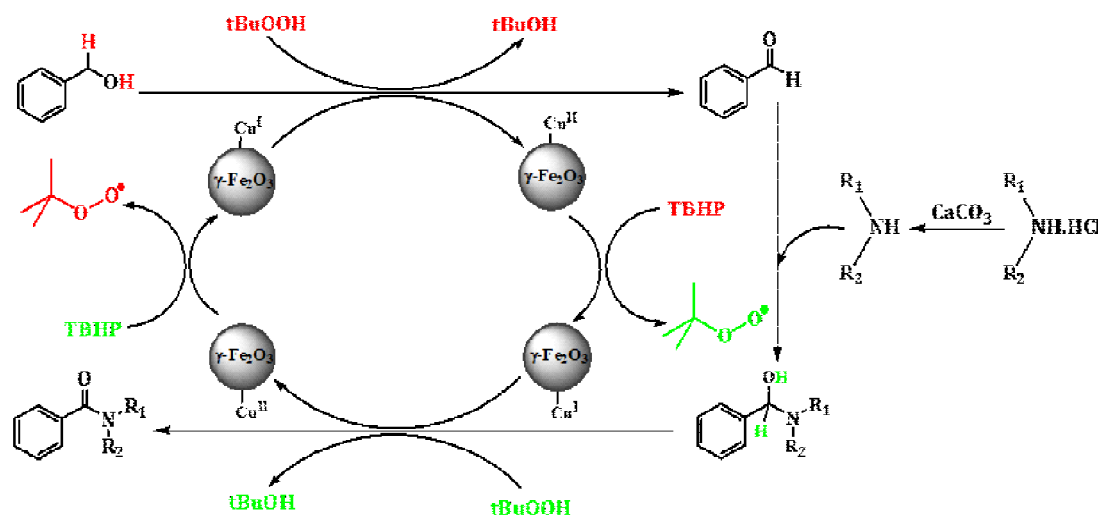
donating group. For benzyl alcohols with electron-donating substituent, oxidation to acid is faster than amidation. All these products were characterized by recording melting points (in some cases), IR, ¹H NMR and ¹³C NMR spectra.

Characterization data of selected products:

1a: ¹H NMR (400 MHz, CDCl_3) δ : 7.83–7.74 (m, 2H), 7.52–7.43 (m, 1H), 7.43–7.35 (m, 2H), 6.57 (s, 1H), 5.91 (ddt, J 17.2, 10.2, 5.7 Hz, 1H), 5.23 (dq, J 17.1, 1.5, 1.5 Hz,

1H), 5.15 (dq, J 10.2, 1.5 Hz, 1H), 4.05 (tt, J 5.7, 1.5 Hz, 2H); ¹³C NMR (101 MHz, CDCl_3) δ : 167.5, 134.5, 134.2, 131.5, 128.6, 127.0, 116.6, 42.5.

2a: ¹H NMR (400 MHz, CDCl_3) δ : 7.77 (d, J 7.6 Hz, 2H), 7.51–7.47 (m, 3H), 6.35 (br, 1H, NH), 3.46 (q, J 6.7 Hz, 2H), 1.58 (m, 2H), 1.42 (m, 2H), 0.95 (t, J 7.3 Hz, 3H); ¹³C NMR (101 MHz, CDCl_3) δ : 167.8, 135.0, 131.5, 128.7, 127.1, 40.0, 31.9, 20.4, 14.0.



Scheme 2. Proposed mechanism for the oxidative amidation of benzyl alcohol with amine HCl salt in the presence of $\gamma\text{-Fe}_2\text{O}_3\text{@CuO}$ -TBHP.

1e: ^1H NMR (400 MHz, CDCl_3) δ : 7.79 (dd, J 5.3, 3.3 Hz, 2H), 7.54–7.47 (m, 1H), 7.47–7.39 (m, 2H), 7.39–7.32 (m, 4H), 7.32–7.27 (m, 1H), 6.42 (brs, 1H), 4.65 (d, J 5.7 Hz, 2H); ^{13}C NMR (101 MHz, CDCl_3) δ : 167.5, 138.3, 134.6, 131.7, 128.9, 128.7, 128.1, 127.8, 127.1, 44.3.

1g: ^1H NMR (400 MHz, CDCl_3) δ : 7.41 (s, 5H), 3.46–3.76 (m, 10H); ^{13}C NMR (101 MHz, CDCl_3) δ : 170.4, 135.3, 129.8, 128.5, 127.0, 66.9.

1h: ^1H NMR (400 MHz, CDCl_3) δ : 7.05 (s, 5H), 3.78–3.27 (br s, 8H); ^{13}C NMR (101 MHz, CDCl_3) δ : 170.5, 135.5, 130.0, 128.7, 127.2, 67.0, 48.2, 42.5.

1j: ^1H NMR (400 MHz, CDCl_3) δ : 7.25–7.51 (m, 5H), 4.67 (d, J 71.5 Hz, 1H), 3.71–3.83 (m, 3H), 3.54 (d, J 59.1 Hz, 2H), 2.22 (d, J 48.8 Hz, 1H), 1.90 (d, J 82.5 Hz, 3H); ^{13}C NMR (101 MHz, CDCl_3) δ : 172.8, 169.7, 136.2, 130.2, 128.3, 127.3, 59.2, 52.3, 49.9, 29.4, 25.4.

The proposed mechanism for this reaction is shown in Scheme 3. $\gamma\text{-Fe}_2\text{O}_3\text{@CuO}$ in the presence of TBHP oxidizes benzyl alcohol to benzaldehyde. Hemiaminal, as an intermediate from the reaction of benzaldehyde with free amine, is produced. After that, the produced hemiaminal is oxidized again in redox cycle $\text{Cu(I)}/\text{Cu(II)}$ in the presence of TBHP and finally, amide is achieved (Scheme 2).

To demonstrate the reusability of $\gamma\text{-Fe}_2\text{O}_3\text{@CuO}$, a series of amidation reactions were performed using benzyl alcohol and hydrochloric salts of benzyl amine. After each re-

action the catalyst was easily brought out using an external magnet, washed with ethyl acetate and sonicated in dichloromethane for 10 min to remove any organic impurities. It was then dried at 80°C and reused for the next cycle without further activation. As exemplified in Fig. 5, the catalyst can be reused for four consecutive reaction cycles with consistent activity under the optimized reaction conditions.

Conclusions

This method has several advantageous such as using non-expensive nanocatalyst, and reusable using an external magnetic field, superior activity, and the inherent stability of the catalyst system and good yields of amide products without significant degradation in activity.

Acknowledgements

We gratefully acknowledge from Payame Noor University of Tehran and Mashhad for the financial support of this work.

References

1. S.-Y. Han and Y.-A. Kim, *Tetrahedron*, 2004, **60**, 2447.
2. C. A. G. N. Montalbetti and V. Falque, *Tetrahedron*, 2005, **61**, 10827.
3. E. Valeur and M. Bradley, *Chem. Soc. Rev.*, 2009, **38**, 606.
4. S. Bahn and S. Imm, *Amination of Alcohols*, 2011, **3**, 1853.
5. Ch. Chen and S. H. Hong, *The Royal Society of Chemistry*, 2011, **9**, 20.

Hassani *et al.*: Formation of amides from alcohols and amines using maghemite-copper oxide nanocomposite as catalyst

6. For selected reviews, see: (a) V. R. Pattabiraman and J. W. Bode, *Nature*, 2011, **480**, 471; (b) C. L. Allen and J. M. J. Williams, *Chem. Soc. Rev.*, 2011, **40**, 3405; (c) S. Roy, S. Roy and G. W. Gribble, *Tetrahedron*, 2012, **68**, 9867.
7. N. A. Owston, A. J. Parker and J. M. J. Williams, *Org. Lett.*, 2007, **9**, 3599.
8. T. Zweifel, J. V. Naubron and H. Grützmaier, *Angew. Chem. Int. Ed.*, 2009, **48**, 559.
9. K. Shimizu, K. Ohshima and A. Satsuma, *Chem. Eur. J.*, 2009, **15**, 9977.
10. (a) Y. Wang, D. Zhu, L. Tang, S. Wang and Z. Wang, *Angew. Chem. Int. Ed.*, 2011, **50**, 8917; (b) J.-F. Soule, H. Miyamura and S. J. Kobayashi, *J. Am. Chem. Soc.*, 2011, **133**, 18550; (c) S. Klitgaard, K. Egeblad, U. V. Mentzel, A. G. Popov, T. Jensen, E. Taarning, I. S. Nielsen and C. H. Christensen, *Green Chem.*, 2008, **10**, 419.
11. For reviews, see: (a) C. L. Allen and J. M. J. Williams, *Chem. Soc. Rev.*, 2011, **40**, 3405; (b) C. Chen and S. H. Hong, *Org. Biomol. Chem.*, 2011, **9**, 20; (c) G. E. Dobereiner and R. H. Crabtree, *Chem. Rev.*, 2010, **110**, 681.
12. E. Rancan, F. Aricò, G. Quartarone, L. Ronchin and A. Vavasori, *Res. Chem. Intermediat.*, 2015, **145**, 939.
13. H. Morimoto, R. Fujiwara, Y. Shimizu, K. Morisaki and T. Ohshima, *Org. Lett.*, 2014, **16(7)**, 2018.
14. C. H. Chen and S. Hyeok Hong, *Org. Biomol. Chem.*, 2011, **9**, 26.
15. H. Xu, X. Qiao, S. Yang and Z. Shen, *J. Org. Chem.*, 2014, **79**, 4414.
16. S. Dutta, S. Sharma, A. Sharma and R. K. Sharma, *ACS Omega*, 2017, **6**, 2778.
17. G. E. Dobereiner and R. H. Crabtree, *Chem. Rev.*, 2010, **110**, 681.
18. S. L. Ch. Ghosh, J. S. Y. Ngiam *et al.*, *Tetrahedron Lett.*, 2013, 4922.
19. K. Semba, T. Fujihara, J. Terao and Y. Tsuji, *Tetrahedron*, 2015, **71**, 2183.
20. W. J. Jang, W. L. Lee, J. H. Moon, J. Y. Lee and J. Yun, *Org. Lett.*, 2016, **18(6)**, 1390.
21. L. Ma'mani, M. Sheykhan, A. Heydari, M. Faraji and Y. Yamini, *Applied Catalysis A: General*, 2010, **377**, 64.
22. R. Etefagh, S. M. Rozati, E. Azhir, N. Shahtahmasebi and A. S. Hosseini, *Scientia Iranica*, 2017, **24(3)**, 1717.
23. R. K. Sharma, R. Gaur, M. Yadav and A. K. Rathi, *ChemCatChem*, 2015, **7(21)**, 3495.
24. S. K. Rajabi, Sh. Sohrabnezhad and S. Ghafourian, *J. Solid State Chem.*, 2016, **244**, 160.
25. R. Bonyasi, M. Gholinejad, F. Saadati and C. Nájera, *New J. Chem.*, 2018, **42**, 3078.

